Gigabit per Second Data Transfer in High-Gain Metamaterial Structures at 60 GHz

Steven J. Franson, *Senior Member, IEEE*, and Richard W. Ziolkowski, *Fellow, IEEE*

***Abstract*—While much metamaterial research has concentrated on the exotic physical properties of metamaterial structures and their potential applications, there has been little reported on the usefulness of these metamaterial structures in actual applications, for example, in communications systems. Moreover, since many metamaterials are designed for operation at very specific frequencies, there are reasonable concerns for how they will act when they are applied to high-data-rate systems. This paper takes a zero-n grid structure that has been shown previously to produce high directivity in the microwave regime, and demonstrates its usefulness for real wireless data transfer in the millimeter-wave regime. The design frequency is selected to be 60 GHz, where there is a large swath of worldwide available bandwidth. An improvement in the overall system gain with no degradation of its gigabit per second data transfer is demonstrated.**

***Index Terms*—High-gain antennas, metamaterials, millimeter-waves, wide-bandwidth communications.**

I. Introduction

DIRECTIVE antenna structures, such as those reported by Enoch *et al.* in [1], appear to have a high potential for use in many communication systems. Of particular interest, within the millimeter-wave spectrum, are their applications to automotive radar, broadband point-to-point communications, and millimeter wave imaging. Enoch *et al.* have demonstrated that a simple three dimensional grid of metallic traces can achieve *ultra-refraction* [2], [3], i.e., they presented a metamaterial having an index of refraction, n, which is positive, but less than one. Additional interesting effects occur as the index approaches zero and a zero-n type of metamaterial is realized [4]–[9]. Of particular interest to high directivity applications, Snell's law tells us that a near zero-n material would cause an electromagnetic wave propagating away from a source within it in any direction to refract almost parallel to the normal of the surface of this material as the wave leaves it. [1].

There have been a number of recent reports that describe highly directive antenna systems based upon a variety of substrate and superstrate configurations [10]–[22]. Many of these concepts stem from the seminal paper [23]. Enoch *et al.* [1]–[3] created their ultra-refractive structure by printing a metallic grid on a foam substrate, and then stacking several of these layers together. They then inserted a monopole antenna (the end of a coaxial line) and measured the resulting radiation pattern. This structure achieved a reported high level of directivity.

One of the primary motivations for attempting to extend these concepts into the millimeter-wave regime is the potential benefit of creating a highly directive, low probability of intercept (LPI) communication system. The design frequency was selected to be 60 GHz, around which there is a large swath of worldwide available bandwidth. This paper examines the use of these grid structures as a metamaterial superstrate for a planar patch antenna at 60 GHz to achieve a higher gain antenna without the need for a large array of these planar elements. Moreover, in contrast to the earlier efforts, the focus here is not on the increase in directivity, but rather on the increase in the overall system gain, which is the real quantity of interest in any practical system. While other 60-GHz antenna systems with interesting directivity and bandwidth have been proposed, e.g., the folded dipole with a high dielectric constant superstrate (fused silica) considered in [24], the use of a zero-n metamaterial superstrate is emphasized here.

In addition, this effort also considers the behavior of a data stream as it propagates through the metamaterial. There have been few reports other than the numerical study in [25] that have considered the impact of a realized metamaterial on the fidelity of the data encoded on a signal propagating through it. Knowledge of the behavior of data as it propagates through a metamaterial is crucial for any potential communications system application. The experimental results reported here will demonstrate that this millimeter-wave high-gain metamaterial-based antenna is useful for real wireless data transfer, i.e., an improvement in the overall gain of the system with no degradation in its gigabit per second data transfer rate is demonstrated. Thus, these results illustrate the usefulness of such a metamaterial superstrate in an actual communication system.

II. Zero-n Grid Structure Superstrate to Achieve High Directivity

There are many physical configurations that could be used as an antenna superstrate. Based on the zero-n grid structures discussed in Enoch [1], Zhu [12], and Weng [18], a wide variety of millimeter-wave metamaterial structures were conceived to act as superstrates. They were all simulated with CST Microwave Studio to predict their gain performance, and the best of these potential designs are reported below. It must be noted that treating these superstrates as having a zero index of refraction (zero-n) behavior is just one of many possible explanations

Manuscript received February 22, 2008; revised January 07, 2009. First published August 04, 2009; current version published October 07, 2009. The work of R. W. Ziolkowski was supported in part by DARPA Contract HR0011-05-C-0068.

S. J. Franson was with Motorola Labs, Millimeter-Wave Research, Tempe, AZ 85284 USA. He is now with Microwave Systems, Crane Electronics Group, Chandler, AZ 85226 USA (e-mail: steve.franson@ieee.org).

R. W. Ziolkowski is with the Department of Electrical and Computer Engineering, University of Arizona, Tucson, AZ 85721 USA (e-mail: ziolkowski@ece.arizona.edu).

Color versions of one or more of the figures in this paper are available online at http://ieeexplore.ieee.org.

Digital Object Identifier 10.1109/TAP.2009.2029277

and methods for designing these structures. Nevertheless, the description of the grid superstrate structure as being a near zero-n medium is justifiable, as the authors have shown in [26] through both parameter extraction techniques, as well as phase propagation behaviors.

Because of its conformal nature, a microstrip patch antenna was elected as the excitation element for the grid. The patch antenna was constructed on an liquid crystal polymer (LCP) substrate, a relatively new substrate material that is becoming popular for very high frequency designs. The material has a relative permittivity $\varepsilon_r = 3.16$ and a loss tangent equal to 0.004 at 60 GHz. The patch antenna was an inset fed design, the microstrip feedline being 254 μm (10 mils) wide. The width of the patch was 1473.2 μm (58 mils), and its length was 1346.2 μm (53 mils); the inset slot was 101.6 μm (4 mils) wide and 482.6 μm (19 mils) long. The predicted gain was 5.193 dBi at 61 GHz; the measured gain was 5.0 dBi at 63 GHz. It was determined that the increase in the resonance frequency was caused by undercutting of the patch during the etching process.

The various metamaterial-based superstrate designs were then integrated with the patch antenna to increase its directivity. However, because the superstrate is placed in the immediate near field of the radiating element, it was expected that the superstrate would detune the antenna. On the other hand, it was in fact desired to create a structure that could be placed over the existing patch antenna and enhance its directivity, without necessarily having to redesign and refabricate the patch, i.e., that it could be used as a superstrate for other planar antenna choices.

A preliminary examination of the effects of a superstrate on the patch antenna performance was achieved by simulating the system as a patch antenna with a piece of foam on top of it. The foam material was Arlon FoamClad 100, a lightweight, foam-based low-loss dielectric that is available as a double-sided copper laminate. The relative permittivity is $\varepsilon_r = 1.30$, and its loss tangent is 0.004. The foam thickness is 1092.2 μm (43 mils); the copper thickness is 35.56 μm (1.4 mils). Even though this foam material has a dielectric constant close to that of air, i.e., foam, without any metallization, will downshift the resonance frequency, increase the mismatch loss, and skew the radiation pattern. Consequently, it was determined that the superstrate structures need to be designed with an air gap above the antenna in order to avoid significantly changing its resonance frequency.

A 7×7 grid superstrate, two-layer structure was first placed directly over the patch antenna. As noted above, this placement has the effect of detuning the antenna. The predicted overall gain was only 8.301 dBi at 60 GHz. In this configuration, the antenna would have to be optimized along with the structure. Again, we emphasize that it was desired to convert the existing low-gain antenna into a high-gain antenna without redesigning the patch antenna. The superstrate structure was then modified in several different ways in an attempt to avoid redesigning the antenna. The optimized period of all of the grids that were investigated was approximately 70 mils.

It was found that detuning the antenna could be avoided by adding space between the grid and the patch. The single layer grid, spaced at a distance of one substrate thickness above the antenna (43 mils $\sim \lambda_0/4.58$), increased the predicted maximum gain to 11.86 dBi. This single-layer air-spaced superstrate performed much better than either the one- or two-layer grid superstrate that was placed directly on top of the antenna. As an alternative to have spacing between the structures, a superstrate concept where a cutout for the transmission line and the patch antenna was created in the bottom layer. Note that only the areas of the bottom layer that were close to the patch or to the transmission line were removed. This configuration, however, did not work as well as just leaving a slab of space between the patch and the grid.

Another superstrate configuration that was considered included a gap equal to 2 foam substrate layer thicknesses (86 mils $\sim \lambda_0/2.29$), which was inserted between the grid superstrate and the patch antenna. In addition, the grid layer was inverted so that the metallization on the foam was now closest to the patch antenna. This configuration worked the best of any of the single layer structures, giving a maximum gain of 12.1 dBi. It also exhibited a fairly broad bandwidth. In contrast to this two-layer structure, another single layer configuration was studied because it was felt that it could potentially lower manufacturing costs. It required that two metallization layers be printed on either side of one layer of the foam substrate. The maximum gain was 14.6 dBi, which was only 0.2 dBi less than the corresponding two-foam-layer structure.

To illustrate that the grid structure has an index of refraction near zero, the extraction approaches described in [27] and [28] were applied to the normal incidence transmission and reflection coefficients, which were obtained numerically with ANSOFT's High Frequency Structure Simulator (HFSS), for a symmetrized (looking the same from each port), infinite version (unit cell in a PEC-PMC waveguide) of the two-layer, 70-mil period, 10-mil trace structure. The magnitudes of S_{11} and S_{21}, the extracted relative permittivity and permeability values and the extracted real and imaginary parts of the refractive index, are shown in Fig. 1. The grid structure exhibits a plasma frequency near 54 GHz in its relative permittivity, which is approximately 0.5 at 60 GHz. The relative permeability is less than one, which can be associated with the fact that the structure is a multi-layer inductive FSS structure. The effective index of refraction is smaller than one throughout the entire frequency band of interest, approximately from 57 GHz to 63 GHz, i.e., $\sim 10\%$. The superstrate is almost completely impedance matched to free space at the resonance frequency.

While the grid superstrate structure has been described as having a near zero index of refraction, the overall system should be viewed as an aperture antenna. Fundamental limits on the antenna directivity dictate that the maximum directivity that can be achieved for this structure would be limited by the overall size of the grid, i.e., if the physical area of the aperture is A, then $D_{\max} = 4\pi A/\lambda^2$, where λ is the wavelength of the source. Therefore, in order to increase the directivity even more, the grid size needed to be increased. Our simulations showed that a 9×9 grid structure can achieve over 16 dBi of gain, while an 11×11 grid structure can achieve over 17 dBi of gain as shown in Fig. 2. On the other hand, beyond the size of an 11×11 grid structure, there was no observed increase in the gain. In fact, going from an 11×11 grid structure to a 13×13 grid structure,

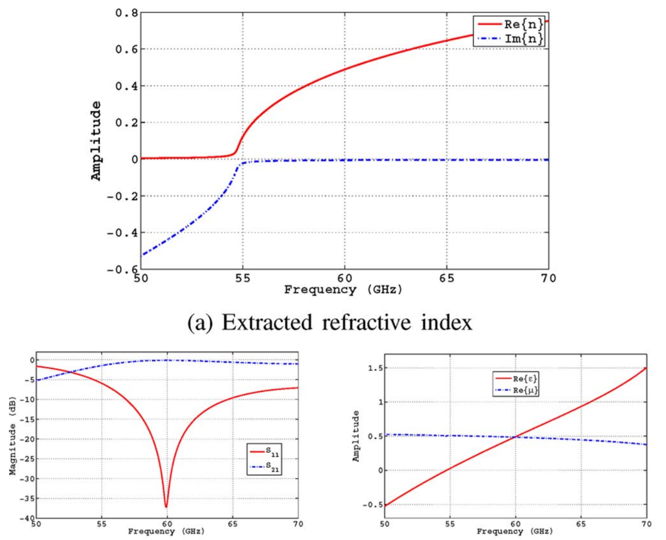

(a) Extracted refractive index

(b) S parameters

(c) Extracted material parameters

Fig. 1. Extracted parameters for the symmetrized, infinite version of the two layer grid structure.

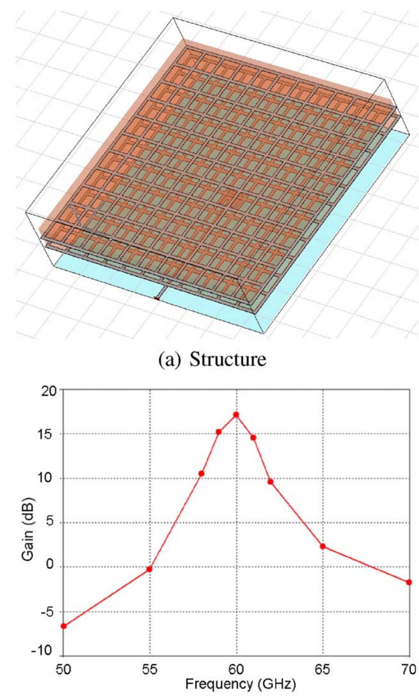

(a) Structure

(b) Gain

Fig. 2. Results for an 11×11 grid structure on two foam layers, optimized in CST with lossless materials.

there was an actual decrease in gain of 0.2 dBi. We believe this was due to the patch antenna becoming too small relative to the overall size of the aperture, i.e., the patch could not efficiently illuminate enough of the superstrate to achieve a benefit from the extra aperture area. In the same sense, because the phase of the illumination at the bottom surface of the grid layer plays a role in the maximum directivity; i.e., the zero-n index slab would effectively translate the phase on its input interface to its output interface, then if the patch is too small to uniformly illuminate that surface, the output surface would not have a uniform phase distribution and, hence, would lead to a smaller maximum directivity.

We found that the optimum superstrate structure, which is shown in Fig. 2, was a two-layer 11×11 grid, which exhibited a maximum gain of 17.2 dBi. It should be noted, however, that these simulations were performed with lossless materials. Again, losses have a major impact at millimeter-wave frequencies unless an ultra-low-loss material is used. Therefore, the structure was resimulated with realistic material parameters. Even with this ultra-low-loss foam material, it caused around 1.1 dB of overall loss, with about one third of this being caused by the metal and the rest being caused by the dielectric. While oblique incidence effective material values were not obtained, we simulated the variation in the gain when the 9×9 grid structure was shifted in the lateral direction by up to 40 mils in either direction, in 10-mil increments. It was found that there was very little change in the gain observed with these variations, thus indicating that precise alignment of the grid structure is not a critical factor in the overall performance of the system and that there is little variation in the effective material properties for the obliquely incident fields.

We note that if the grid size needs to be increased in order to increase the gain, one might ask why we simply did not elect to just use an array of patches to achieve the desired increase in gain. The answer lies in the high loss of the substrate at millimeter-wave frequencies. A microstrip array of patch antennas would employ some type of feed network, which becomes very lossy with increasing array size. Therefore, large patch arrays are generally not desirable at millimeter-wave frequencies.

After finding the optimized grid size for the superstrate structure, a few other variations were also studied. For instance, we investigated a grid structure which has the metal traces oriented only in one direction, i.e., a set of metallic strips. In theory, the Drude response of the grid structure should arise only from traces that are parallel to the electric field. Thus, these "lines" should have a similar response to that of the grid structure when the patch antenna is polarized correctly. Indeed, with the correct orientation, it was found that the gain was only 0.8 dB less than with the complete crossed grid structure of the same size.

Due to the acquisition of enhanced computing resources which were optimized for REMCOM's XFDTD software, the simulations at this stage of our investigations were moved from CST into this enhanced XFDTD simulation environment. The only drawback was that in contrast to CST, there was no automated parameterization or optimization schemes available in XFDTD. The XFDTD software, which predicted a higher gain value than CST for the patch antenna, also predicted a higher gain value for the optimized structure. Each simulation required on the order of 100 000 time steps to reach steady state and a -60 dB convergence value. We were able to run each with a very fine mesh (i.e., with a cubical cell whose side length was 0.5 mils), but with a Courant limited time step of 34.59 fs. This led to very long simulation run times. Nonetheless, because of the higher resolution available in the XFDTD simulations enabled by the enhanced computing resources, we believe they were more accurate than the CST values.

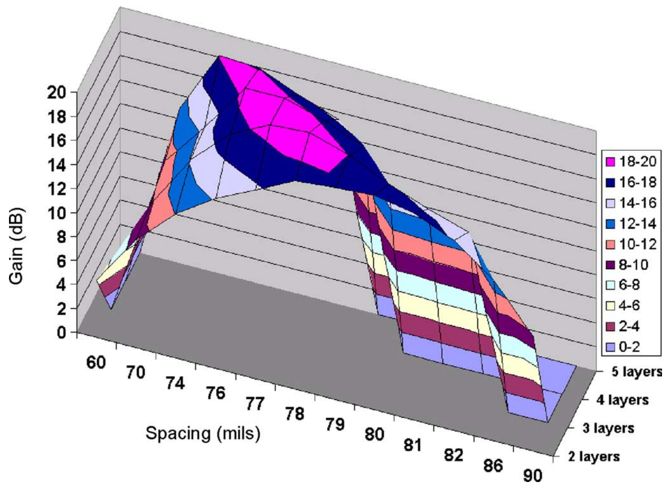

Fig. 3. Three-dimensional plot of the variation of the gain as a function of the number of layers and the grid-antenna spacing.

Fig. 3 shows a three-dimensional plot of the gain as a function of both the spacing between the patch antenna and the bottom of the superstrate, and the number of layers. This XFDTD data was obtained for the grid structure with a period equal to 70 mils. As shown in Fig. 4, the maximum gain value for the optimized zero-n grid superstrate-patch antenna system was approximately 19 dBi. This optimized value was approximately a 13-dBi improvement in gain over that of the corresponding patch antenna simulation value.

Another unfortunate aspect of these XFDTD simulations from the user standpoint was that single frequency simulations had to be run to obtain the radiation characteristics, while a separate simulation had to be run to predict the frequency response of the reflection coefficient. Therefore, it was not initially evident during the optimization process that the structure was indeed detuning the antenna and, hence, causing the reflection coefficient to be large, even when the gain was optimal. Consequently, after the optimization was complete, the overall system efficiency of the antenna system (which includes mismatch and other losses) that is driven by a 50-Ω source was determined to be only 40.8% at the peak gain frequency of 61 GHz. A second optimization series was then performed, taking into account the system efficiency. It included modifying the patch antenna dimensions to achieve the best match to the source. A maximum gain of 16 dBi with an overall system efficiency of 63% was thus achieved. These results were obtained for a grid structure with a period of 68 mils, four layers, and a 70-mil spacing between the patch and the first grid layer.

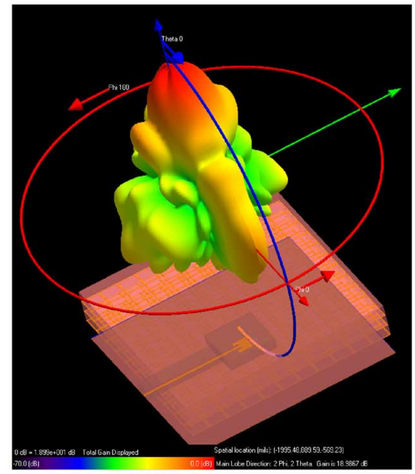

(a) Structure and 3D radiation pattern

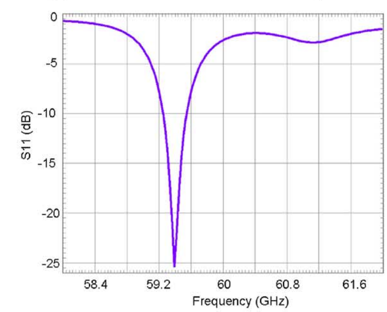

(b) S11

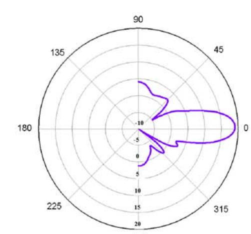

(c) 2D Radiation Pattern: $E_\phi(dB)$, $\phi = 0°$

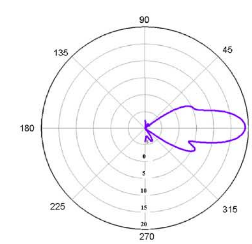

(d) 2D Radiation Pattern: $E_\theta(dB)$, $\phi = 90°$

Fig. 4. Results for the grid structure superstrate optimized in XFDTD to achieve the best overall gain value.

III. Zero-n Grid Structure Experimental Results

A. General Fabrication and Measurement Issues

Layouts for several of these grid structures and the resulting zero-n superstrates were created so that they could be fabricated and tested. The fabricated single layer 11×11 grid structure that had a 70-mil period is shown in Fig. 5. The metal patterning looked very good, with only a slight rounding of the internal edges. The layers were constructed with an adhesive backing so that they could be attached easily to each other to form a multilayer substrate.

The first attempted measurement of a grid metamaterial superstrate-based antenna was actually the 7×7 grid structure having a 70-mil period. The patch antenna and the grid are shown in Fig. 6. The patch antenna was held down using Kapton tape, which was measured to be a consistent 2.5 mils thick. This thickness is important, because it will further separate the patch antenna from the foam. The 7×7 grid structure is shown with two supports, made from two layers of the foam, in order to get the desired separation.

When building the multi-layer structure, an important issue was noticed. When the adhesive release layer was removed, the foam immediately curled up. The result of this behavior was to make the foam no longer planar. As shown in Fig. 7, when looking at the edge of the 2 layer structure, there was significant curvature. The exact measure of curvature was difficult to obtain. It was on the order of 10 mils, but it was certainly more

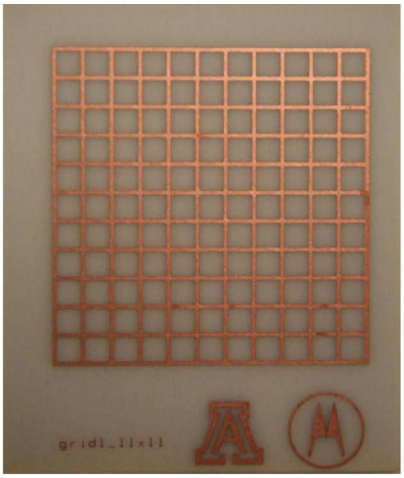

(a) Entire grid layer

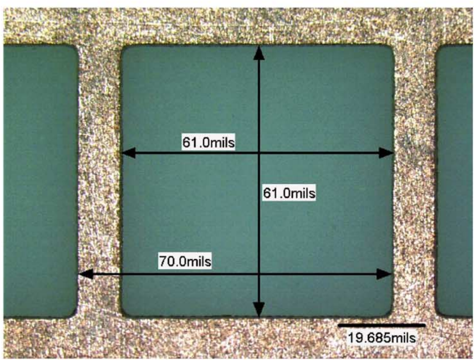

(b) Microscope view of one of the grid elements, including dimensions

Fig. 5. Fabricated 70-mil grid structure.

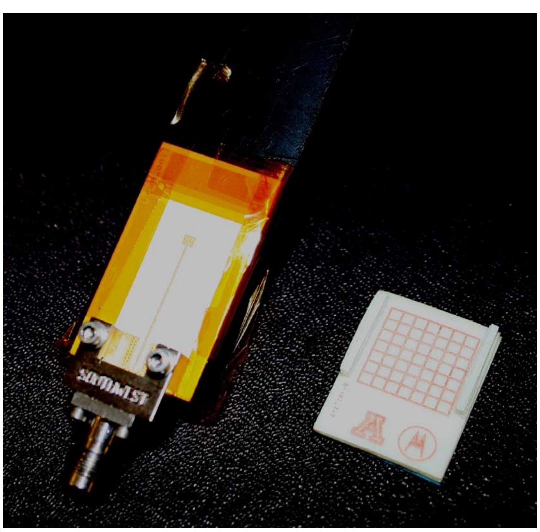

Fig. 6. Fabricated patch antenna and one layer of the foam-based 7 × 7 grid structure.

than our critical dimension of 1 mil. The effects of this issue will be discussed at the end of this section.

It should be noted that we were using a coaxial end launch connector on our patch antenna, which interfaces to a coplanar waveguide-to-microstrip transition. Consequently, there was actually a length of transmission line leading to the patch antenna.

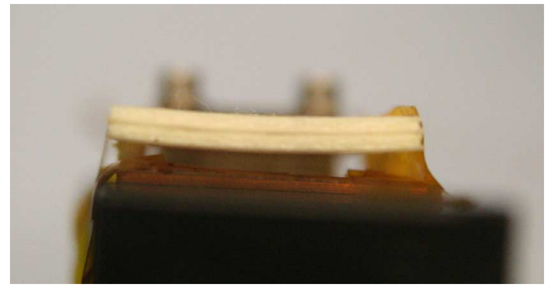

Fig. 7. Edge view of the 7 × 7 grid superstrate-based patch antenna, showing the undesired curvature.

In order to understand the gain measurements reported here, it must remain clear as to what parts of the system were included in the measurement, i.e., what components were de-embedded using the calibration. For the VNA used in our measurements, only a waveguide calibration kit was available. Therefore, a coaxial-to-waveguide adapter was included in the calibration. This meant that the true reference point was not at the end of the coaxial cable. If the assumption is made that our coaxial connector has similar loss characteristics to that of the waveguide adapter, then the connector is essentially calibrated out. This is accurate enough for our magnitude-only calibration; however, there is some room for error when using this connector. The only edge launch connectors available are rated up to 50 GHz; however, they work well enough up to 60 GHz. The alignment of the pin to the microstrip track, however, is critical. Moreover, the coaxial-to-microstrip transition is not explicitly de-embedded from the measurement. Therefore, with a moderate amount of accuracy, we can say that our gain measurements include the loss in the transmission line, as well as the mismatch of the transmission line. This means that we were actually measuring the system gain of the antenna *and* the feedline. This is an important distinction, as many authors only report directivity or antenna gain, as opposed to the actual realized *system gain*. This turns out to be especially important for the grid structure, i.e., it can be difficult to optimize for good gain and low reflection loss simultaneously. An additional note of importance is that the transmission line loss was included in the XFDTD simulations. However, the difference between the *net input power* and the *available power* must be subtracted out of the simulation results in order to compare the results to the measured system gain.

B. *Measured Results*

The following two subsections will focus on the optimized measurements of the fabricated antenna structures. Those structures were the 70-mil and 68-mil period designs discussed in the previous section. An important point to understand regarding these measurements was that they were tuned to achieve the best overall system gain. In particular, the various system parameters, e.g., the antenna and superstrate spacing, and so forth were adjusted to realize the maximum received signal as viewed on the network analyzer. The dimensions were so critical that it was not possible to get good results without this tuning. For instance, just by adjusting the pressure of the tape holding the foam to the LCP substrate, the results could change dramatically. Of course, this was due to the small tolerances allowed in

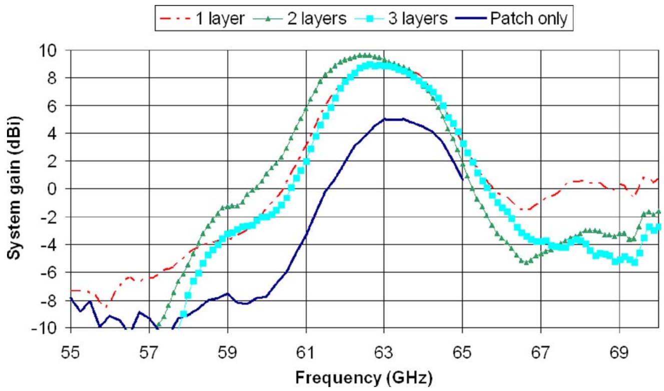

Fig. 8. Measured frequency response of the 70-mil period grid superstrate-based patch antenna.

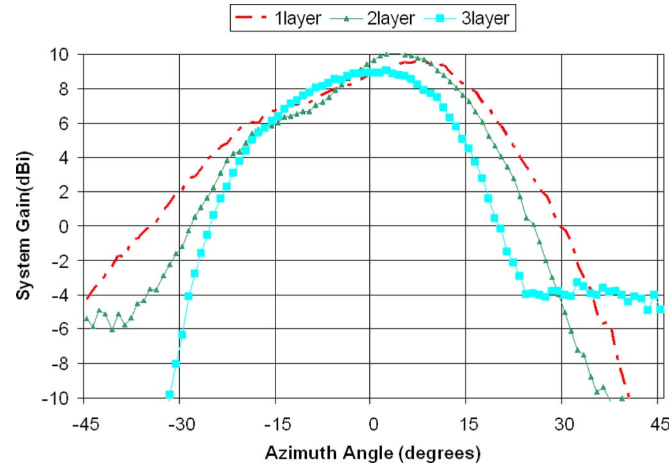

Fig. 9. Measured azimuth response of the 70-mil period grid superstrate-based patch antenna at the frequency of maximum gain.

the design parameters. Even the thickness of the tape (2.5 mils) holding down the patch antenna substrate was significant. The adjusted pressure and positioning of the tape not only tuned the spacing, but had an effect on the thickness of the flexible foam material and the curvature of the antenna. The actual optimum spacing between the foam and the LCP was different depending on the number of layers used, and the results showed a reoptimized structure for each configuration.

1) 70-Mil Period Design: The three-layer 70-mil period grid structure superstrate had the highest gain of the simulated structures. A difficulty in both the design and measurement was that it was not matched very well at the frequency showing the highest gain. This is contradictory to many antenna designs, in which you can optimize the antenna to minimize the reflection coefficient and then expect it also to have the optimum gain. In building these millimeter-wave structures, it became very evident that the frequency of resonance could be significantly shifted depending on the spacing between the foam and the LCP.

The 70-mil period design was optimized in the simulations for a height of the superstrate above the patch antenna that was thought to be convenient, i.e., two substrate thicknesses. To achieve this design in practice, two unclad pieces of the foam were attached together to realize a spacer between the foam-based grids and the LCP, with a cutout to produce the desired air gap. As discussed above, there was additional spacing provided by the tape that secured the LCP to the test fixture; it also had an impact on the tuning of the system. The frequency response of the gain is shown in Fig. 8 for the varying number of layers. With one layer, the gain achieved at boresight was 8.98 dBi, while for the two- and three-layer structures, gains of 9.63 and 8.96 dBi, respectively, were achieved. Therefore, the first and second layers clearly provided more gain as expected. Unfortunately, the addition of the third layer actually decreased the gain in contrast to the simulation results. An explanation of this anomaly will be given below. The original antenna gain of the 63-GHz patch antenna system was 4.99 dBi. The measured azimuthal radiation pattern of the tuned superstrate structure, which were taken at the frequency of highest gain, is shown in Fig. 9.

2) 68-Mil Period Design: The 68-mil period XFDTD optimized grid structure was also fabricated and tested. For this antenna system, the optimal design called for a 70-mil gap between the foam and the LCP. In order to achieve this, a 70-mil thick piece of rigid foam was obtained from a different manufacturer. A piece of foam that was matched to the grid size was cut out, and then additional cuts were made to create the air gap opening for the antenna and the transmission line to avoid detuning. The results of this grid structure were slightly better than those produced by the 70-mil grid structure. At boresight, the system gain was measured to be 9.53, 10.31, and 10.56 dBi for one, two, and three layers, respectively. The azimuthal radiation pattern was taken at the frequency of highest gain. At 4 degrees off in elevation, a system gain of 11.09 dBi was measured, which is the highest system gain we achieved with these structures. Tuning of the four-layer structure was attempted, but a higher gain was not achieved as predicted by the simulations. This too will be discussed further below.

C. Comparison of Experimental and Simulated Results

In general, there were a variety of discrepancies between the measured and simulated results. Nonetheless, in general, these measurements were a success, as high-gain responses were achieved for even the single layer structures. Unfortunately, the anticipated increases in the overall gain when the number of grid layers was increased was not as large as was expected. Many factors, including the simulated feed width, the curvature of the substrate, and the thickness of the foam layers, contributed towards these differences.

One major discrepancy was in the results for the gain versus the number of layers. While a measurable high gain was achieved for one, and sometimes two grid layers. the antenna performance began to degrade for an increasing number of layers. One possible explanation was discussed earlier, i.e., the curvature of the layers that resulted from the adhesive issues. The poor tolerances of the foam substrate thickness also had a significant impact. Another issue was the presence of a layer of polyester that holds the metallization to the foam. The individual characteristics of the polyester and the foam were unknown; and, consequently, they could not be simulated accurately. What was provided by the manufacturer is a composite permittivity that gives the average response of the material. Also, the material parameters are not explicitly known at 60 GHz, which was another area of risk for this design. In the end we found this gain-layer number discrepancy was due to a combination of several factors.

One contribution was a variation in the layer thickness. In order to investigate the actual thickness variations, a few layers of the substrate were attached to each other and measured under a high power microscope. The results are shown in Fig. 10, in which different cross sections of this stack are shown. The thickness was less than advertised by the manufacturer. As one can see from Fig. 10(c), the measured sample in fact had a variation in thickness of almost 4 mils across a very short distance. Furthermore, there are noticeable variations between adjacent metallizations, and they were clearly not in the same plane. These measurements were convincing evidence that the material variations were a major cause of the discrepancies between the simulations and experiments. To confirm this hypothesis, measurements and new simulations were done to represent the fabricated antenna structure.

The next photographs given in Fig. 11 show the actual structure that was expected to provide the best system gain. This was the four-layer structure with the 68-mil period. Measurements were made with a microscope on the layers of the structure to compare them with the expected thickness of 43 mils. Examining the figure, the structure that touches the LCP was constructed from a more rigid, 70-mil-thick foam. This material actually did measure 70 mils and would have been a good choice with which to construct the entire design. Unfortunately, the material is not currently available in a copper clad version that could be processed. The next distance measured was that of the glue layer, holding the foam rigid. It was found that there was a gap formed by the glue and air, which ranged from 10 mils up to a 20 mils in thickness; this gap can be seen on the edges of the structure. Moving to the flexible foam layers, several measurements were taken along the outer edges. The first, second, and third layers had variations between 36 and 39 mils, with each layer having an average thickness of 38 mils. The fourth layer, however, had variations from 30 to 37 mils, with an average of 35 mils.

It was clear that the deviation from the simulated thickness may have resulted in the less than anticipated gain performance of the multilayer superstrate-based antennas. Nonetheless, a question remained: Was it the change in the thickness that affected the results, or was it the variability in thickness across each layer? Simulations were run with these variations in order to determine their effects. For the three-layer structure, the nominal expected system gain was 13.46 dBi, whereas the measured results were 10.31 dBi. When the thickness of the layers was decreased to 38 mils, the numerically predicted system gain was only 7.35 dBi, which was significantly lower than our measured results. This, however, was actually an unfair comparison. As stressed earlier, the spacing of all of the measurements was tuned to achieve the best system gain. Therefore, we had to relook at what the best gain would be for the 38-mil-thick layer structure when the spacing was varied. In particular, the spacing was adjusted in 1 mil (25.4 μm) increments and these simulation results showed that the system gain could be adjusted as high as 14.15 dBi, which is actually a higher value than predicted by the original simulations. Assuming that the tuning method which we used was accurate enough to position the superstrate to within 1 mil of the design distance, these

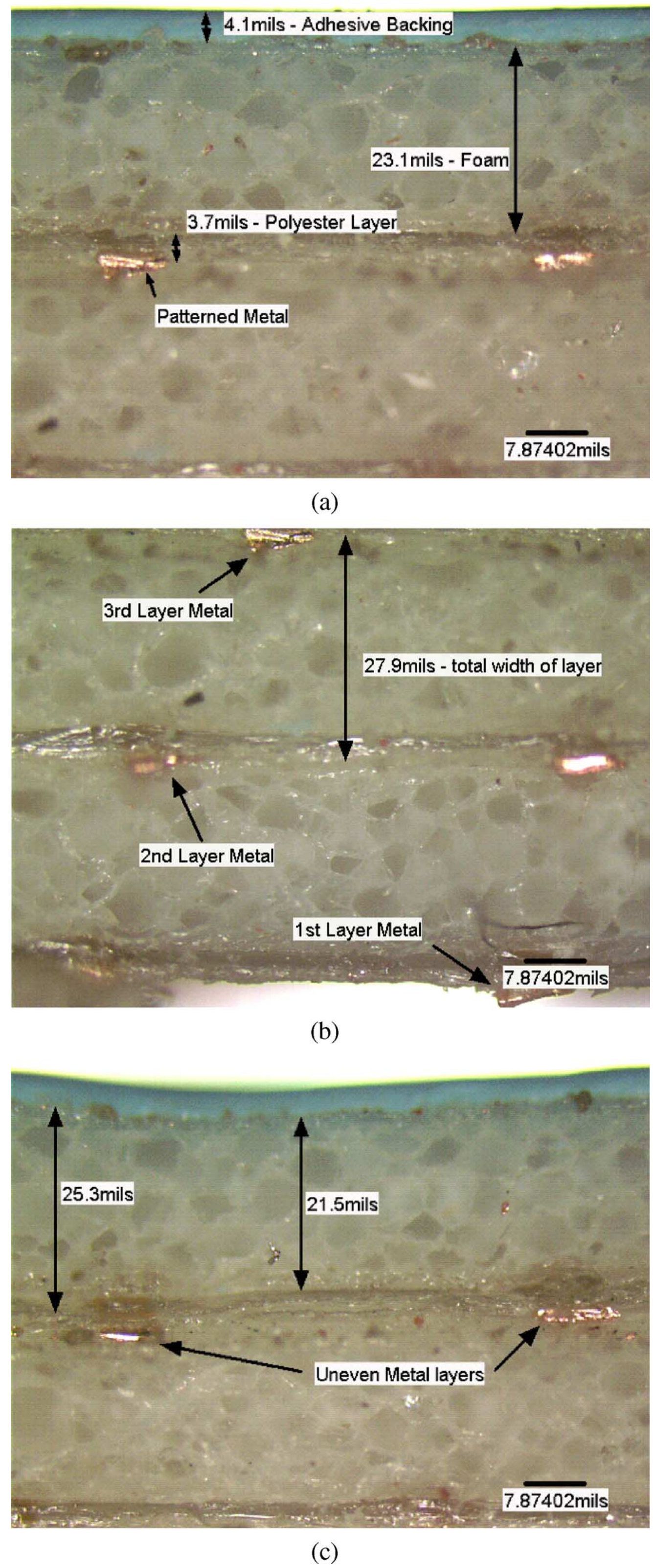

Fig. 10. Edge view of a foam stack-up: (a) cut 1; (b) cut 2; and (c) cut 3.

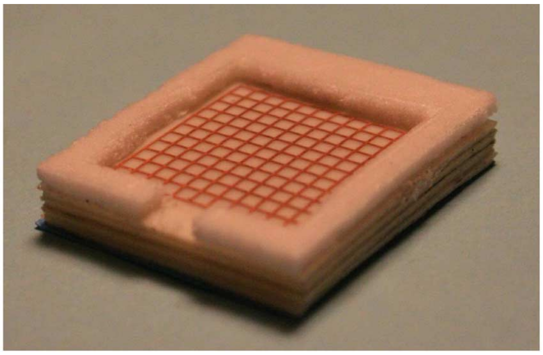

(a) Perspective view

(b) Edge view

Fig. 11. Four-layer grid-based superstrate structure.

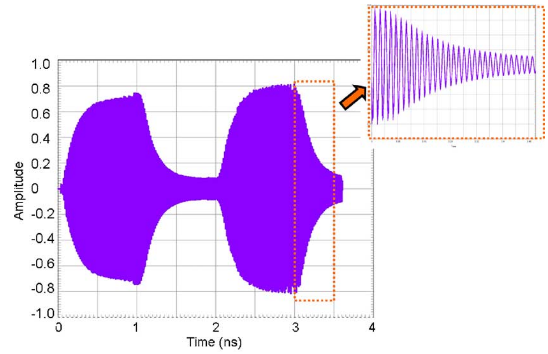

(a) 1 Gb/s

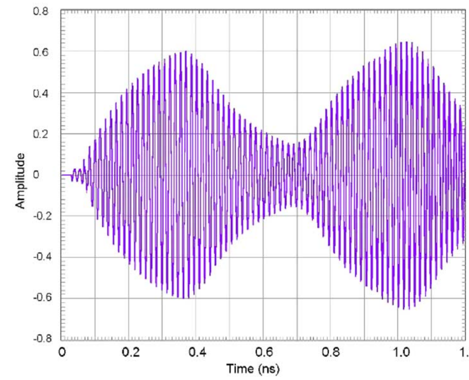

(b) 3 Gb/s

Fig. 12. Simulated signals generated by a patch antenna excited with several high-data-rate OOK modulated sources. The amplitudes are relative to that of the input signal.

simulations seemed to disprove that the change in the average thickness was the cause of the lower gain. The four-layer structure, however, exhibited different variations. Recall that the fourth layer averaged only 35 mils. What then is the effect of having a layer that is different from the others? Simulations showed that the best system gain achievable for such a modified four-layer structure, even with optimal tuning, would only be 12.34 dBi. This is a lower gain than the three-layer structure. These results provide the best explanation as to why there was a decrease in the antenna gain when the fourth layer was added to the system. Having layers with different thicknesses does significantly degrade the performance of this type of antenna system.

It is, of course, unreasonable to measure exactly all of the variations in the grid thickness or curvature, or even to try to simulate them. Nevertheless, our simulation results show how variations in general can significantly degrade the overall gain performance of the 60-GHz superstrate-based patch antenna systems. Curvatures or changes in thickness as little as 1 mil can have a definitive affect on the overall system performance. The current material system is obviously incapable of holding the design tolerances required for millimeter-wave frequencies. However, even though the structures did not meet the simulated performances, significant and useful gain was still achieved. Increasing the gain of an antenna from 5 to 11 dBi can have a significant effect on the link margin of many practical systems. Also, we again note that this is a measure of the overall system gain; it includes the losses of the transmission line which would account for an additional 2 dB. Despite the discrepancies between the simulations and experiments, the end result was that we were able to demonstrate that these zero-n superstrate enhanced antenna systems do have useful gain. We thus moved forward to the experiments discussed in the next section which further demonstrated their usefulness for multi-gigabit communication systems.

IV. Simulated Modulation Results

In order to demonstrate what the signal fidelity limitations of the grid-based superstrate are when it is integrated with the patch antenna, it was first necessary to understand the time domain response of the patch antenna itself. Patch antennas are well-known narrowband radiators. The responses of the 60-GHz LCP patch antenna alone to different data rate ON–OFF key (OOK) stimuli are shown in Fig. 12. These 1- and 3-Gb/s OOK results show how the ON–OFF ratio of an amplitude modulated signal degrades with increasing data rate for a fixed patch size. The actual maximum data rate would be determined by many factors, including the sensitivity of the receiver, the linearity of the transmitter, multi-path interference, and so forth. The simulation data indicates that it is possible for multi-gigabit operation to be achieved with a patch antenna.

Once the response of the patch antenna was obtained for a given input signal, the corresponding response of the expected worst case grid structure was then calculated. The four-layer 68-mil grid period superstrate structure had both the highest expected system gain, as well as the highest number of layers of any of the optimized antennas. We were interested not only in the main lobe response, but also in the response at the nulls in order to see if there was any unintended radiation present, particularly in the pattern null directions. The nulls of this structure were in both the $\phi = 90^\circ$, $\theta = 38^\circ$ and the $\phi = 0^\circ$, $\theta = 27^\circ$ directions with expected values of -15 and -9.4 dBc, respectively. The simulation results for the output signals in these directions are given in Fig. 13. They show that the main lobe signal

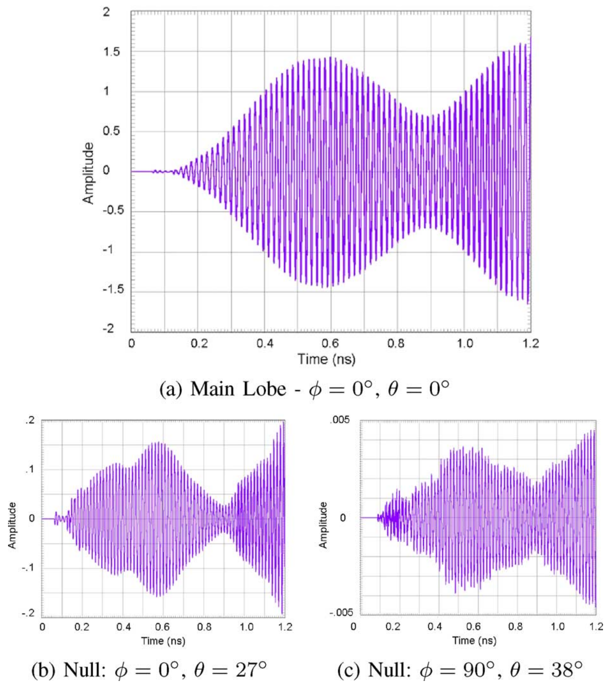

Fig. 13. Output signal of the zero-n superstrate-based patch antenna driven by a 3-Gb/s OOK modulated signal.

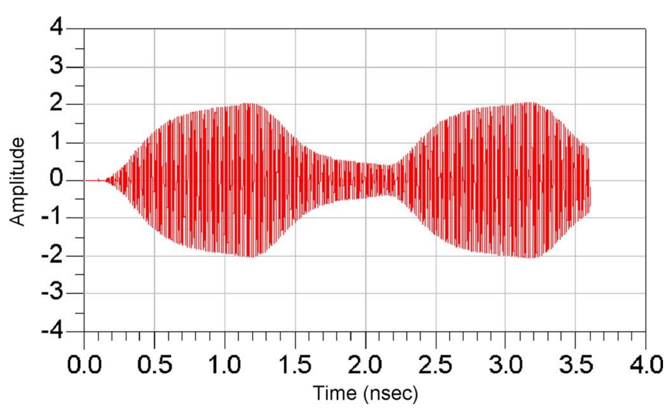

Fig. 14. Output signal of the zero-n superstrate-based patch antenna driven by a 1-Gb/s OOK modulated signal.

for the zero-n superstrate-based patch antenna has a signal behavior that is similar to that of the patch by itself. They also show that in the deepest null direction ($\phi = 90°$, $\theta = 38°$), there is very little energy present throughout a cycle. On the other hand, in the $\phi = 0°$, $\theta = 27°$ direction, there is some weak signal that does not exactly follow the original modulation. The 1 gigabit per second (1-Gb/s) excitation signal shown in Fig. 14 fared much better as expected, yielding a higher ON–OFF ratio than the higher 3-Gb/s data rate signal.

It was anticipated that a phase (BPSK) modulated source would produce properties that are similar to those generated by the OOK excitation. The disruption of the steady state fields by the phase transitions exhibit effects that mimic those associated with the OOK coding. The BPSK simulations confirmed the anticipated similarities.

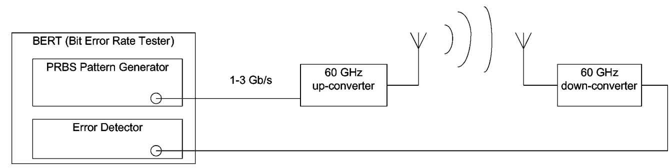

Fig. 15. System setup for the BERT measurements.

Fig. 16. Transmitter and receiver setup for the BERT measurements. The transceivers were placed less than 1 m apart for this test.

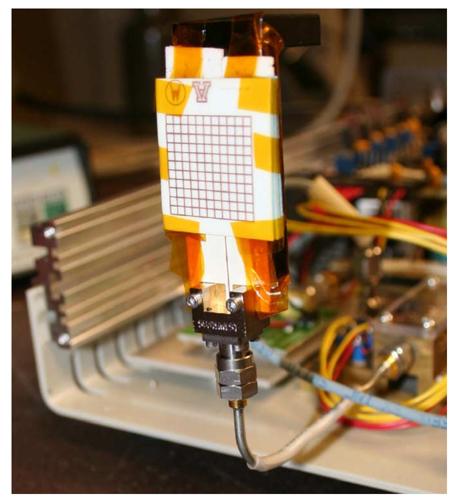

Fig. 17. View of the antenna under test for the BERT measurements.

V. Experimental Modulation Results

Because the simulations predicted that they would not significantly lower the bandwidth of the patch antennas, the zero-n superstrate-based antenna systems were tested with actual data transmissions. In particular, bit error rate (BER) testing of the 63-GHz patch antenna with the two-layer grid-based superstrate having a grid period of 68 mils, and the 57-GHz patch antenna with the two-layer grid-based superstrate having a grid period of 70 mils was performed. In order to measure the bit error rate of these systems, they were removed from the antenna chamber. While still attached to the antenna chamber mounting structure, they were inserted into a 60-GHz wireless system. A block diagram of the BERT is shown in Fig. 15. The experimentally measured 70-mil structure is shown in the test setup in Figs. 16 and 17. The receive module is shown on the left-hand side of Fig. 16 and is configured with a horn antenna. On the other hand, the transmit antenna on the right-hand side has been replaced with the new antenna. The local oscillator on the transmit side was adjusted to 57 or 63 GHz, depending on the antenna under test.

The 63-GHz patch antenna was first connected in the BERT system as described. The maximum data rate of the system was determined, and the corresponding eye diagrams were captured. Eye diagrams are simply a time domain response of the system

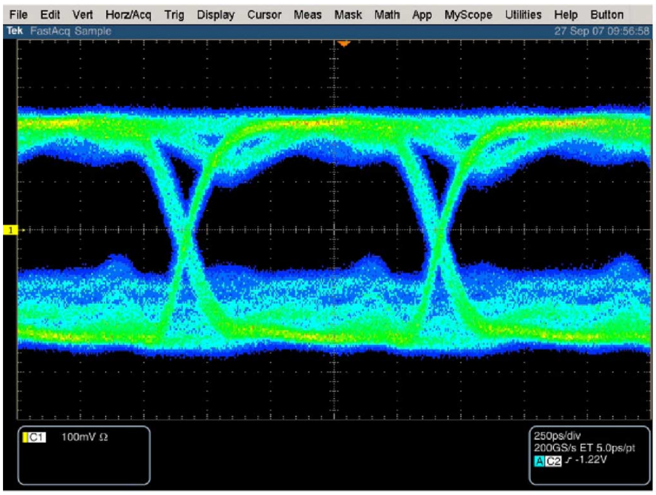

Fig. 18. Measured eye pattern of the patch antenna driven by a 1-Gb/s signal.

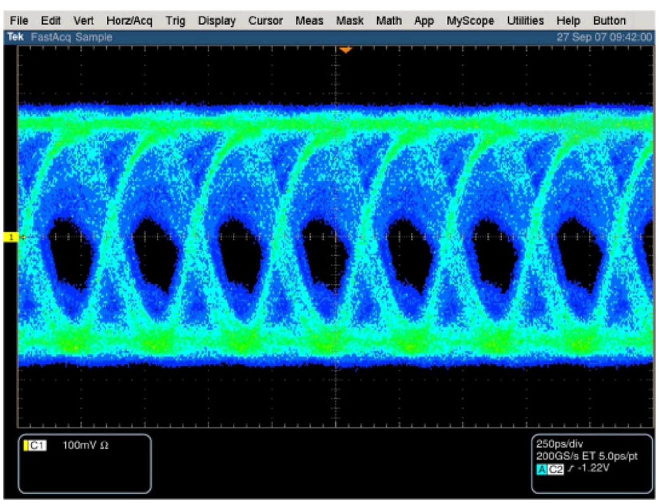

Fig. 19. Measured eye pattern of the patch antenna driven by a 3-Gb/s signal.

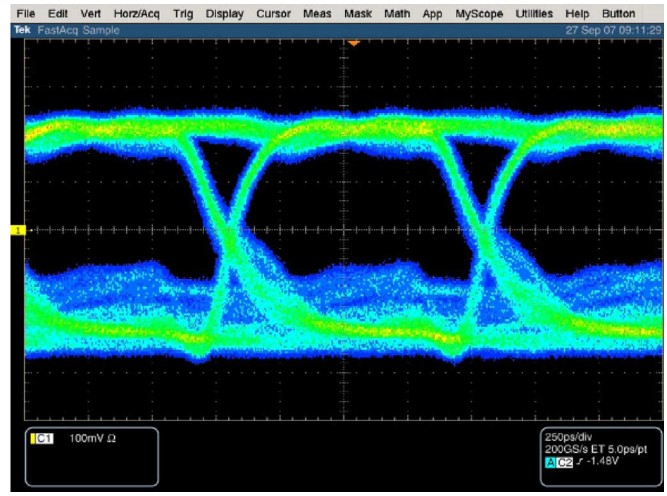

Fig. 20. Measured eye pattern generated by the two-layer grid (68-mil period) superstrate-based patch antenna driven with the 1-Gb/s signal.

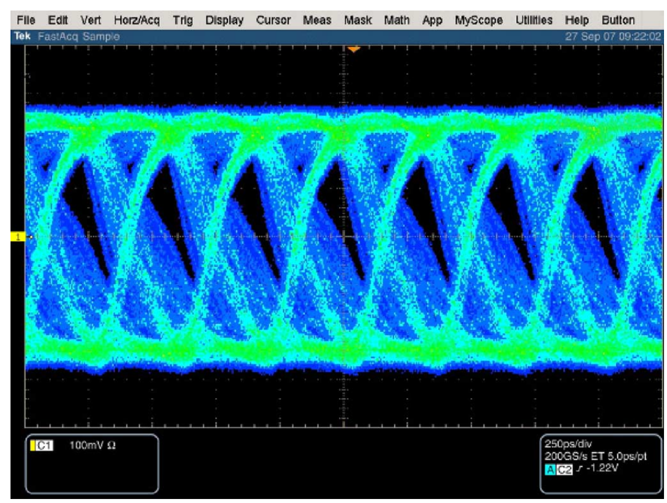

Fig. 21. Measured eye pattern generated by the two-layer grid (68-mil period) superstrate-based patch antenna driven with the 3-Gb/s signal.

with the oscilloscope triggered from the clock signal. The result is an overlay of many portions of the data stream. When there is a possibility of error free transmission, an "eye" or gap in the picture is formed. The larger the eye opening, the more margin there is for error free data transmission. Figs. 18 and 19 show the resulting eye diagrams of the patch antenna for the 1- and 3-Gb/s data rate signals. It should be noted that in both cases there is some distortion in the eye, notably an increase in the "zero level." There is also some intersymbol interference, which is an artifact of the transmitter and is not related to the antenna performance. As shown, the eye becomes closed near 3 Gb/s, indicating that this is the maximum data rate that can be transmitted by the tested zero-n superstrate-based patch antenna. Indeed, the BERT results showed that there is error free transmission (defined here as greater than $1\mathrm{E}+12$ bits without an error) up to 3 Gb/s, dropping off drastically after that point, with a total loss of synchronization at 3.3 Gb/s. It should be stressed that the 1E12 bit error rate is measured, i.e., 1E12 bits were transmitted across the link, and all bits were correctly received. This is much better than any typical current communication system would require. The input pattern used for all the measurements was a pseudorandom bit stream (PRBS) of length 2^7-1, meaning that there are a maximum of seven consecutive ones or zeros in the data stream.

The effect of adding the two-layer grid structure superstrate over the patch antenna was examined next. Figs. 20 and 21 show the measured eye diagrams when two layers of the 68-mil period grid were placed approximately 70 mils above the patch antenna. While the second layer enhanced the gain as expected, its effect on the data rate, and therefore the bandwidth, was almost unnoticeable. The shape of the eye did change some, but the maximum error free data rate remained at 3 Gb/s. These results prove that it is possible to design a transceiver using these highly directive metamaterial-enhanced antenna systems for multi-gigabit per second data rates.

This important result was demonstrated a second time using the 70-mil period two-layer grid superstrate-based antenna having the foam support underneath the grids. As shown in Fig. 17, the grids were held together by tape. In this case, however, in addition to showing that the resulting grid superstrate-based patch antenna can support rates up to 3 Gb/s, the eye diagram and pattern-triggered time domain waveform are shown, respectively, in Figs. 23 and 22 for a source signal

Fig. 22. Measured time domain response generated by the two-layer grid (70-mil period) superstrate-based patch antenna excited by a 1.25-Gb/s signal.

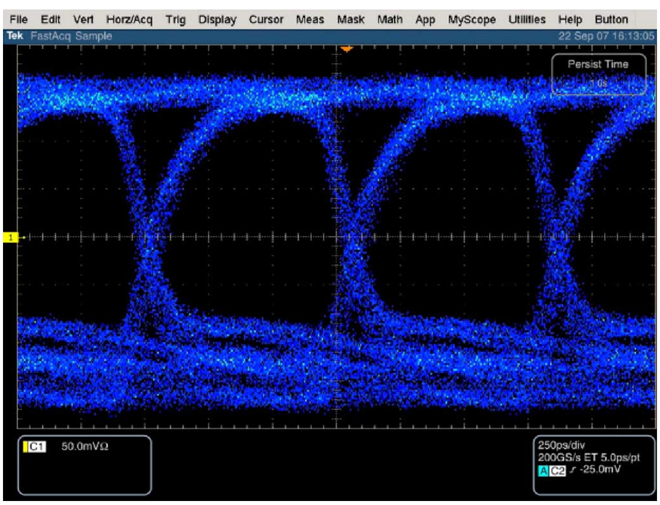

Fig. 23. Measured eye pattern of the two-layer grid (70-mil period) superstrate-based patch antenna excited by a 1.25-Gb/s signal.

having a data rate of 1.25 Gb/s. From a practical point of view, the data rate of 1.25 Gb/s is of particular interest. It is the rate at which serial Gigabit Ethernet is transmitted (1 Gb/s of data plus 0.25 Gb/s of overhead).

The transmitter and receiver systems in this configuration were then connected by a serial Gigabit Ethernet signal as shown in Fig. 24. Gigabit Ethernet on Cat5 cable from a standard computer was output as four parallel lines of data, which were then converted into a serial stream of data by means of a media converter. Data was then transmitted successfully between the two computers that were connected to them. This means that the metamaterial-based antenna structure transmitted real data over a wireless channel at 1.25 Gb/s, with no degradation when compared to the same results obtained from a wired link. Given the enhanced gain of the antenna systems, these results demonstrate that the grid superstrate structure can create a significant increase in the system gain for gigabit per second signals in the 60-GHz ISM band.

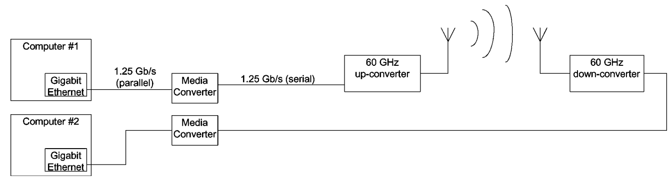

Fig. 24. System setup for the Gigabit Ethernet transfer between two computers.

VI. Conclusion

In this paper, we have introduced several high-gain, zero-n, grid-based superstrates that were integrated with a microstrip patch antenna at 60 GHz. The simulations of these superstrate designs, which included the loss of the feedline, showed antenna gains as high as 19 dBi. These structures were fabricated on sheets of a flexible, low-loss foam, copper laminate material, and their performances were measured. The single layer structures performed very well, but the multi-layer structures were plagued by the non-uniformity in the thickness of the foam layers, as well as other material and fabrication issues. The highest system gain achieved, which includes *both* the feedline and mismatch loss, was just over 11 dBi. These discrepancies were examined in detail. It was shown by measuring the cross-sections of the foam substrates and through supporting simulations, that the available materials clearly did not have high enough tolerances for detailed millimeter-wave designs that require precise dimensions, i.e., on the order of $+/-1$ mil (25.4 μm).

Even though the gain predicted in our simulations was not achieved in practice due to those fabrication issues, a useful and significant amount of gain was achieved nonetheless with these zero-n structures. This was verified experimentally using a real high-data-rate communications system. Not only did our experimental results using these high-gain structures demonstrate that the composite antenna system had the same bandwidth and high-data-rate transmitting/receiving capabilities as the patch antenna alone, they also verified actual 1.25-Gb/s data transfer over a 60-GHz wireless link between two computers. These experimental results showed conclusively that the zero-n metamaterial superstrate-based antenna systems reported here are useful for multi-gigabit communication systems. Both our BER and data transfer tests showed zero data loss or corruption, and no noticeable decrease in the system performance. In practice, these high-gain antenna systems are more favorable at millimeter-wave frequencies than using a patch array because of the high losses associated with the requisite array feed network.

Several lessons were learned as the zero-n grid structures were designed and fabricated for operation in the 60-GHz ISM band. They include the following.

1) The patch antenna should be optimized with the grid in order to maximize the overall system gain.
2) A rigid material system should be used with at least $+/-$ 1 mil thickness tolerance.
3) A homogeneous material should be used instead of a foam substrate with polyester layers.

4) A multi-layer material system should be used rather than manually attaching the layers. (LTCC could be used, but its high dielectric constant and losses at these frequencies may be prohibitive. A substrate such as Alumina could be used, but it is not inherently a multi-layer material system.)
5) Access to a simulator with sufficient computing power and features, including automated parametrization, optimization, swept frequency capabilities, and swept gain measurement capabilities is critical to the design and verification process and should be obtained initially.

Addressing these issues will lower the risks of future designs and will lead to even more successful implementations of these antennas in the future. While it was demonstrated that the zero-n metamaterial structure and its use as a patch antenna superstrate would be useful for high-data-rate antenna applications at 60 GHz, further work will be needed in order to demonstrate an easily fabricated structure for commercial applications at millimeter-wave frequencies.

REFERENCES

[1] S. Enoch, G. Tayeb, P. Sabouroux, N. Guérin, and P. Vincent, "A metamaterial for directive emission," *Phys. Rev. Lett.*, vol. 89, 2002, paper 213902.

[2] G. Tayeb, S. Enoch, P. Vincent, and P. Sabouroux, "A compact directive antenna using ultrarefractive properties of metamaterials," in *Proc. Int. Conf. Electromagn. Adv. Applicat. (ICEAA'03)*, Torino, Italy, Sep. 08–12, 2003, pp. 423–426.

[3] D. R. Maystre, S. Enoch, and G. Tayeb, "Ultrarefraction and negative refraction in metamaterials," *Proc. SPIE*, vol. 5359, pp. 64–64, 2004.

[4] R. W. Ziolkowski, "Propagation in and scattering from a matched metamaterial having a zero index of refraction," *Phys. Rev. E*, vol. 70, Oct. 2004, paper 046608.

[5] A. Alù and N. Engheta, "Achieving transparency with plasmonic and metamaterial coatings," *Phys. Rev. E*, vol. 72, Jul. 2005, paper 016623.

[6] J. B. Pendry, D. Schurig, and D. R. Smith, "Controlling electromagnetic fields," *Science*, vol. 312, pp. 1780–1782, 2006.

[7] A. Alù, M. G. Silveirinha, A. Salandrino, and N. Engheta, "Epsilon-near-zero metamaterials and electromagnetic sources: Tailoring the radiation phase pattern," *Phys. Rev. B*, vol. 75, Apr. 2007, paper 155410.

[8] B. Edwards, A. Alù, M. E. Young, M. G. Silveirinha, and N. Engheta, "Experimental verification of epsilon-near-zero metamaterial coupling and energy squeezing using a microwave waveguide," *Phys. Rev. Lett.*, vol. 100, Jan. 2008, paper 033903.

[9] R. Liu, Q. Cheng, T. Hand, J. J. Mock, T. J. Cui, S. A. Cummer, and D. R. Smith, "Experimental demonstration of electromagnetic tunneling through an epsilon-near-zero metamaterial at microwave frequencies," *Phys. Rev. Lett.*, vol. 100, Jan. 2008, paper 023903.

[10] B.-I. Wu, W. Wang, J. Pacheco, X. Chen, T. Grzegorczyk, and J. A. Kong, "A study of using metamaterials as antenna superstrate to enhance gain," *Progr. Electromagn. Res.*, vol. PIER 51, pp. 295–328, 2005.

[11] A. R. Andrew, K. P. Esselle, B. C. Sanders, and T. S. Bird, "High-gain 1-D EBG resonator antenna," *Microw. Opt. Technol. Lett.*, vol. 47, pp. 107–114, Oct. 2005.

[12] F. Zhu, Q. Lin, and J. Hu, "A directive patch antenna with a metamaterial cover," in *Proc. Microw.Conf./Asia-Pacific Conf. (APMC)*, 2005, vol. 3.

[13] A. P. Feresidis, G. Goussetis, S. Wang, and J. Y. C. Vardaxoglou, "Artificial magnetic conductor surfaces and their application to low-profile high-gain planar antennas," *IEEE Trans. Antennas Propag.*, vol. 53, no. 1, pp. 209–215, Jan. 2005.

[14] A. Ourir, A. de Lustrac, and J.-M. Lourtioz, "All-metamaterial-based subwavelength cavities ($\lambda/60$) for ultrathin directive antennas," *Appl. Phys. Lett.*, vol. 88, Feb. 2006, paper 084103.

[15] E. Saenz, I. Ederra, R. Gonzalo, and P. de Maagt, "Enhancement of the power radiated by a dipole antenna at boresight by means of a left handed superstrate," in *Proc. IEEE Int. Workshop Antenna Technol. Small Antennas Novel Metamaterials (IWAT 2006)*, White Plains, NY, Mar. 6-8, 2006, pp. 9–12.

[16] P. Lee, Y. J. W. Yeo, and R. Mittra, "Directivity enhancement of printed antennas using a class of metamaterial superstrates," *Electromagn.*, vol. 26, pp. 203–218, 2006.

[17] Y. Vardaxoglou and F. Capolino, "Review of highly-directive flat-plate antenna technology with metasurfaces and metamaterials," in *Proc. 36th Eur. Microw. Conf.*, Manchester, U.K., Sep. 2006, pp. 963–966.

[18] Z.-B. Weng, N.-B. Wang, Y.-C. Jiao, and Y.-C. Zhang, "A directive patch antenna with metamaterial structure," *Microw. Opt. Tech. Lett.*, vol. 49, pp. 456–459, Feb. 2007.

[19] P. M. T. Ikonen, E. Saenz, R. Gonzalo, and S. A. Tretyakov, "Modeling and analysis of composite antenna superstrates consisting on grids of loaded wires," *IEEE Trans. Antennas Propag.*, vol. 55, pp. 2692–2700, Oct. 2007.

[20] Y. Ge and K. P. Esselle, "Designing high gain microwave antennas by optimising a FSS superstrate," in *Proc. Eur. Microw. Conf.*, 2007, pp. 412–415.

[21] H. Xu, Z. Zhao, Y. Lv, C. Du, and X. Luo, "Metamaterial superstrate and electromagnetic bandgap substrate for high directive antenna," *Int. J. Infrared Milli. Waves*, vol. 29, pp. 493–498, Mar. 2008.

[22] E. Saenz, R. Gonzalo, I. Ederra, J. C. Vardaxoglou, and P. de Maagt, "Resonant meta-surface superstrate for single and multifrequency dipole antenna arrays," *IEEE Trans. Antennas Propag.*, vol. 56, pp. 951–960, Apr. 2008.

[23] D. R. Jackson and N. G. Alexopoulos, "Gain enhancement methods for printed circuit antennas," *IEEE Trans. Antennas Propag.*, vol. 33, pp. 976–987, Sep. 1985.

[24] T. Zwick, D. Liu, and B. P. Gaucher, "Broadband planar superstrate antenna for integrated millimeterwave transceivers," *IEEE Trans. Antennas Propag.*, vol. 54, pp. 2790–2796, Oct. 2006.

[25] S. J. Franson and R. W. Ziolkowski, "Numerical studies of the interaction of time-modulated multi-gigabit sequences with metamaterial structures at millimeter-wave frequencies," *Int. J. Numer. Model*, vol. 19, pp. 195–213, Mar. 2006.

[26] S. J. Franson and R. W. Ziolkowski, "Confirmation of zero-N behavior in a high gain grid structure at millimeter-wave frequencies," *IEEE Antennas Wireless Propag. Lett.*, vol. 8, pp. 387–390, 2009.

[27] D. R. Smith, S. Schultz, P. Markos, and C. M. Soukoulis, "Determination of effective permittivity and permeability of metamaterials from reflection and transmission coefficients," *Phys. Rev. B*, vol. 65, Apr. 2002, paper 195104.

[28] X. Chen, T. M. Grzegorczyk, B.-I. Wu, J. Pacheco, Jr., and J. A. Kong, "Robust method to retrieve the constitutive effective parameters of metamaterials," *Phys. Rev. E*, vol. 70, Jul. 2004, paper 016608.

Steven J. Franson (M'02–SM'07) received the B.S., M.S., and Ph.D. degrees in electrical engineering at the University of Arizona, Tempe.

He worked as a member of the Millimeter-Wave Applied Research team at Motorola Labs, Chandler, AZ, from 1997 to 2008. His research interests there included 60-GHz communication systems, 77-GHz radar, 94-GHz imaging, and metamaterials. He is currently with Microwave Systems Solutions at Crane Electronics Group, Chandler, AZ.

Richard W. Ziolkowski (M'87–SM'91–F'94) received the Sc.B. degree in physics (*magna cum laude*) with honors from Brown University, Providence RI, in 1974 and the M.S. and Ph.D. degrees in physics from the University of Illinois at Urbana-Champaign, in 1975 and 1980, respectively.

He was a member of the Engineering Research Division at the Lawrence Livermore National Laboratory, Livermore, CA, from 1981 to 1990 and served as the leader of the Computational Electronics and Electromagnetics Thrust Area for the Engineering Directorate from 1984 to 1990. He joined the Department of Electrical and Computer Engineering at the University of Arizona, Tempe, as an Associate Professor in 1990 and was promoted to Full Professor in 1996. He was selected by the Faculty to serve as the Kenneth Von Behren Chaired Professor for 2003 to 2005. He currently is serving as the Litton Industries John M. Leonis Distinguished Professor. He holds a joint appointment with the College of Optical Sciences at the University of Arizona. His research interests include the application of new mathematical and numerical methods to linear and nonlinear problems dealing with the interaction of acoustic and electromagnetic waves with complex media, metamaterials, and realistic structures.

Prof. Ziolkowski is a member of Tau Beta Pi, Sigma Xi, Phi Kappa Phi, the American Physical Society, the Optical Society of America, and Commissions B (Fields and Waves) and D (Electronics and Photonics) of URSI (International Union of Radio Science). He is a Fellow of the Optical Society of America. He has served as a member of the IEEE Antennas and Propagation Society (AP-S) Administrative Committee (ADCOM). He served as the IEEE AP-S Vice President in 2004 and as President in 2005. He served as the Vice-Chairman of the 1989 IEEE AP-S and URSI Symposium, San Jose, CA, and as the Technical Program Chairperson for the 1998 IEEE Conference on Electromagnetic Field Computation. He has served an Associate Editor for the IEEE TRANSACTIONS ON ANTENNAS AND PROPAGATION. He was a Steering Committee Member for the 2004 ESA Antenna Technology Workshop on Innovative Periodic Antennas. He served as a Co-Chair of the International Advisory Committee for the inaugural IEEE International Workshop on Antenna Technology: Small Antennas and Novel Metamaterials (IWAT 2005). He has served as a member of the International Advisory Committees for IWAT 2006–2009 and for MAPE 2005. He served as an Overseas Corresponding Member of the ISAP 2007 Organizing Committee. He served as the Technical Program Committee Chair for the 2008 Metamaterials Congress, Pamplona, Spain. He was a Co-Guest Editor for the October 2003 IEEE TRANSACTIONS ON ANTENNAS AND PROPAGATION Special Issue on Metamaterials. For the U.S. URSI Society, he served as Secretary and as Chairperson of the Technical Activities Committee for Commission B and as Secretary for Commission D. He has served as a Member-at-Large of the U.S. National Committee (USNC) of URSI and is now serving as a member of the International Commission B Technical Activities Board. He was a Co-Guest Editor of a 1998 JOSA A special issue. He was a Co-Organizer of the Photonics Nanostructures Special Symposia at the 1998, 1999, and 2000 OSA Integrated Photonics Research (IPR) Topical Meetings. He served as the Chair of the IPR subcommittee IV, Nanostructure Photonics, in 2001. He was awarded the Tau Beta Pi Professor of the Year Award in 1993 and the IEEE and Eta Kappa Nu Outstanding Teaching Award in 1993 and 1998.